

Effect of pressure and Ir substitution in YbRh_2Si_2

M. E. M. acovei, M. Nicklas, C. Krellner, C. Geibel and F. Steglich

Max Planck Institute for Chemical Physics of Solids, Nothnitzer Str. 40, 01187

Dresden, Germany

E-mail: m.acovei@cpfs.mpg.de

Abstract.

In this article we present a study of the electrical resistivity of $\text{Yb}(\text{Rh}_{1-x}\text{Ir}_x)_2\text{Si}_2$, $x = 0.06$, under high pressure and in magnetic field. Ir substitution is expanding the unit cell and leads to a suppression of the antiferromagnetic transition temperature to zero, where eventually a quantum critical point (QCP) exists. We applied hydrostatic pressure to reverse the effect of substitution. Our results indicate that $\text{Yb}(\text{Rh}_{0.94}\text{Ir}_{0.06})_2\text{Si}_2$ is situated in the immediate proximity to a volume controlled QCP, but still on the magnetically ordered side of the phase diagram. The temperature-pressure phase diagram of $\text{Yb}(\text{Rh}_{0.94}\text{Ir}_{0.06})_2\text{Si}_2$ resembles that of the pure compound. Substitution acts mainly as chemical pressure. Disorder introduced by substitution has only minor effects.

PACS numbers: 74.62.Fj, 71.27.+a, 71.10.Hf, 73.43.Nq, 74.62.Dh

1. Introduction

The unique properties that develop around a quantum critical point (QCP) are a major topic of current solid state research. YbRh_2Si_2 exhibits a weak antiferromagnetic (AFM) transition at atmospheric pressure with a Neel temperature of only $T_N = 70$ mK [1]. By applying a small magnetic field perpendicular to the crystallographic c axis the transition temperature can be continuously suppressed to zero at about $B_c = 60$ mT ($B_c = 660$ mT for $B \parallel c$), driving the system to a QCP [2]. The temperature dependence of the specific heat and resistivity reveal an extended non-Fermi-liquid (NFL) regime around the magnetic field-induced QCP [3]. Under external pressure the Neel temperature is continuously increasing, typical for an Yb-based intermetallic system. The pressure effect on YbRh_2Si_2 has been intensively studied [4, 5, 6, 7]. YbRh_2Si_2 can be tuned to the paramagnetic side of the pressure (volume) controlled QCP by increasing the unit-cell volume. This can be achieved only by chemical substitution. Replacing a nominal concentration of 5 at.% Si by Ge in YbRh_2Si_2 leads to a shift of T_N from 70 mK in the pure compound to $T_N = 20$ mK [3]. A similar result has been reported on small La substitution [8]. Expanding the crystal lattice of YbRh_2Si_2 by substituting Rh with the isovalent Ir, allows one to tune the system through the QCP without significantly affecting the electronic properties. Recent measurements of the magnetic susceptibility

on $\text{Yb}(\text{Rh}_{1-x}\text{Ir}_x)_2\text{Si}_2$ demonstrate that for low Ir doping, $x \leq 0.025$, the system orders magnetically, while in the crystals with 17 at.% Ir substitution, no magnetic transition can be observed [9]. In this work we studied $\text{Yb}(\text{Rh}_{0.94}\text{Ir}_{0.06})_2\text{Si}_2$ supposed to be at the border of magnetism, by means of electrical resistivity measurements as a function of both hydrostatic pressure (p) and magnetic field (B). The substitution of 6 at.% Rh by Ir leads to a lattice expansion of only about 0.03%. Our results provide evidence that $\text{Yb}(\text{Rh}_{0.94}\text{Ir}_{0.06})_2\text{Si}_2$ is situated in proximity to the QCP, but still slightly on the magnetic side of the temperature-volume phase diagram. The T - p phase diagram resembles that of the stoichiometric YbRh_2Si_2 , considering a shift by a rigid pressure corresponding to the lattice expansion due to the 6 at.% Ir substitution.

2. Experimental details

Single crystals of $\text{Yb}(\text{Rh}_{0.94}\text{Ir}_{0.06})_2\text{Si}_2$ were grown from Influx. The sample stoichiometry has been verified by energy dispersive X-ray analysis (EDX). The tetragonal ThCr_2Si_2 crystal structure has been confirmed by X-ray powder diffraction. Measurements of the electrical resistivity have been performed using a standard four-point technique at temperatures 50 mK $\leq T \leq$ 300 K and in magnetic fields up to $B = 8$ T in a physical property measurement system (Quantum Design) and in a $^3\text{He}/^4\text{He}$ dilution refrigerator. The current was applied within the ab plane and the magnetic field parallel to the crystallographic c axis. In the low-pressure region a piston-cylinder type pressure cell capable of pressures up to $p = 3$ GPa with silicone oil as pressure transmitting medium was used. For pressures $p \geq 10$ GPa, a Bridgman-type pressure cell with steatite as

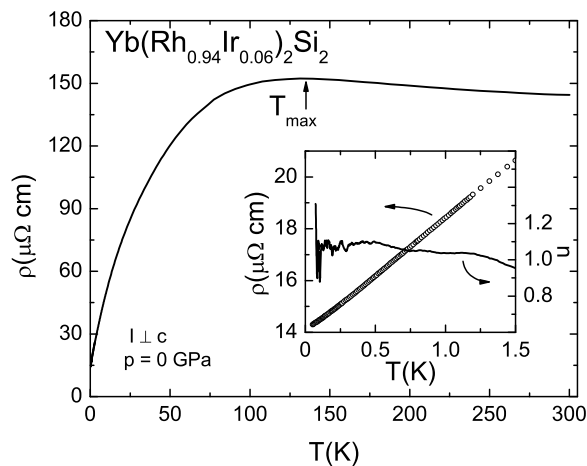


Figure 1. Electrical resistivity of $\text{Yb}(\text{Rh}_{0.94}\text{Ir}_{0.06})_2\text{Si}_2$ at atmospheric pressure measured perpendicular to the c axis as function of temperature. Inset: resistivity (left axis) and temperature exponent $n = d \ln(\rho(T)/\rho(0))/d \ln T$ in the temperature range 50 mK $\leq T \leq$ 1.5 K.

pressure transmitting medium was utilized. The pressure inside the pressure cell was determined by monitoring the pressure dependence of the superconducting transition temperature of Sn or Pb, respectively, placed near the sample inside the pressure cell.

3. Results and discussion

Figure 1 shows $\rho(T)$ at ambient pressure in the temperature range 50 K $\leq T \leq$ 300 K. The electrical resistivity temperature dependence, $\rho(T)$, of $\text{Yb}(\text{Rh}_{0.94}\text{Ir}_{0.06})_2\text{Si}_2$ at atmospheric pressure follows the typical behavior expected for a Kondo-lattice system. Below 300 K the resistivity increases slightly with decreasing temperature, then exhibits a broad maximum around $T_{\text{max}} = 135$ K. Upon further cooling $\rho(T)$ strongly decreases due to the onset of coherent Kondo scattering. In the stoichiometric compound YbRh_2Si_2 , the resistivity maximum at $p = 0$ is reported at about the same temperature [1]. At low pressure $p = 4$ GPa, the resistivity shows a single broad maximum around $T_{\text{max}} = 100$ K (figure 2). Upon increasing pressure the maximum shifts to lower temperatures, indicating a decrease of the hybridization between the Yb 4f and the conduction electrons. For pressures larger than $p = 4$ GPa, a shoulder is developing next to the maximum. At $p = 4.5$ GPa the maximum is observed at $T_{\text{max}}^{\text{low}} = 45$ K and the shoulder at $T_{\text{max}}^{\text{high}} = 95$ K. The pressure responses of the maximum and the shoulder are different: $T_{\text{max}}^{\text{low}}(p)$ shifts to lower temperatures upon increasing pressure, while $T_{\text{max}}^{\text{high}}(p)$ is nearly pressure independent. In pure YbRh_2Si_2 a similar behavior is found, the single maximum at low pressure splits into two at

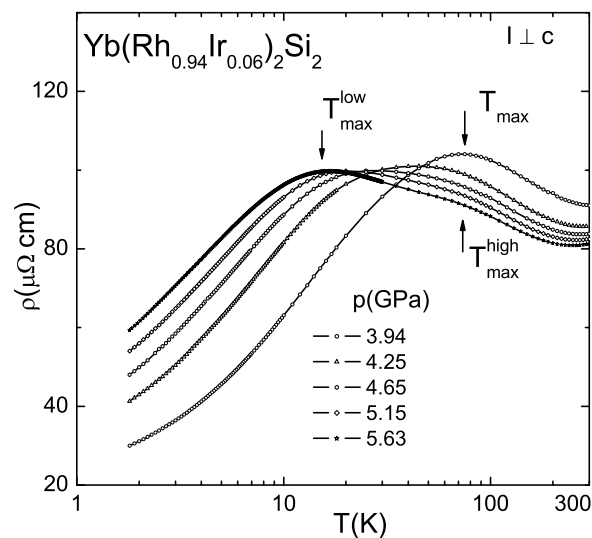


Figure 2. Temperature dependence of the electrical resistivity for $\text{Yb}(\text{Rh}_{0.94}\text{Ir}_{0.06})_2\text{Si}_2$ at different pressures in the temperature range 1 $\leq T \leq$ 300 K. Arrows indicate T_{max} for $p = 3.94$ GPa. For $p = 5.63$ GPa a maximum at $T_{\text{max}}^{\text{low}}$ and a shoulder at $T_{\text{max}}^{\text{high}}$ are clearly distinguishable, both indicated by arrows.

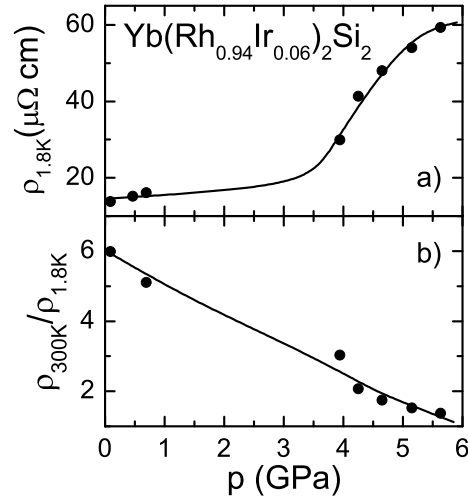


Figure 3. Upper panel: isothermal resistivity at $T = 1.8 \text{ K}$, $\rho_{1.8K}$, as function of pressure; lower panel: pressure dependence of the resistivity ratio $\rho_{300K} = \rho_{1.8K}$. The lines are guides to the eye.

about the same pressure [6]. The single maximum in $\rho(T)$ at low pressures can be explained by a combination of scattering processes on the ground state doublet and on the excited crystalline electric field (CEF) levels. Taking into account the CEF level scheme obtained from inelastic neutron scattering for YbRh_2Si_2 at ambient pressure [10], for $p \approx 4.5$ GPa the high temperature shoulder can be attributed to inelastic Kondo scattering on the excited CEF levels and the low temperature maximum to Kondo scattering on the ground state doublet. The very similar pressure evolution of the high-temperature resistivity in YbRh_2Si_2 and $\text{Yb}(\text{Rh}_{0.94}\text{Ir}_{0.06})_2\text{Si}_2$ indicates that the pressure effect on the CEF levels is comparable in both materials. However, in $\text{Yb}(\text{Rh}_{0.94}\text{Ir}_{0.06})_2\text{Si}_2$ the resistivity maximum is situated at slightly higher temperatures compared with YbRh_2Si_2 . The isothermal pressure dependence of the resistivity at $T = 1.8 \text{ K}$, $\rho_{1.8K}(p)$, stays initially nearly constant with increasing pressure before it strongly increases, above $p \approx 4$ GPa, by a factor of more than 3 (Figure 3a). At the same time the resistivity ratio $R_{1.8K} = \rho_{300K} = \rho_{1.8K}$ decreases monotonically. This reveals that the increase of $\rho_{1.8K}(p)$ above $p \approx 4$ GPa is caused by additional incoherent scattering at low temperatures. A pressure-induced increase of the residual resistivity, ρ_0 , was previously found in different Yb- and Ce-based compounds, like YbIr_2Si_2 [11], YbCu_2Si_2 [12], or $\text{CeCu}_2(\text{Si}_{1-x}\text{Ge}_x)_2$ [13]. Different mechanisms based on magnetic or valence transitions can lead to a strongly elevated ρ_0 . It was found theoretically that in quantum-critical systems impurity scattering can be strongly enhanced by quantum-critical spin-fluctuations [14, 15]. In a theoretical model based on valence-fluctuations a strong increase of ρ_0 and a linear temperature dependence of the resistivity at low temperatures is predicted above a crossover temperature T_v at a valence transition [16]. From the present data it is not possible to decide which mechanism leads to the enhanced

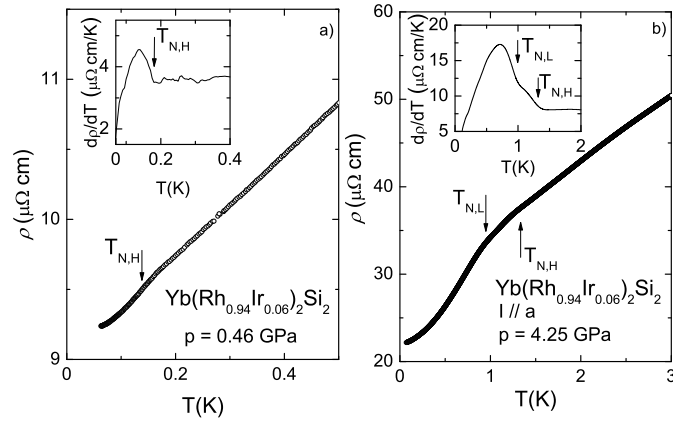


Figure 4. Low-temperature electrical resistivity of $\text{Yb}(\text{Rh}_{0.94}\text{Ir}_{0.06})_2\text{Si}_2$ at a) $p = 0.46$ GPa and b) $p = 4.25$ GPa. The transition temperatures were determined from the temperature derivative of $\rho(T) = d\rho/dT$ as shown in the insets of panel a) and b) for $p = 0.46$ GPa and 4.25 GPa, respectively. The arrows indicate the magnetic transitions at $T_{N,H}$ and $T_{N,L}$, respectively.

ρ_0 in $\text{Yb}(\text{Rh}_{0.94}\text{Ir}_{0.06})_2\text{Si}_2$.

At atmospheric pressure, the low-temperature resistivity of $\text{Yb}(\text{Rh}_{0.94}\text{Ir}_{0.06})_2\text{Si}_2$ shows no anomaly pointing to the existence of a magnetic transition in the temperature range down to $T = 50$ mK (inset figure 1). In magnetic susceptibility measurements a clear magnetic transition was observed for $\text{Yb}(\text{Rh}_{0.975}\text{Ir}_{0.025})_2\text{Si}_2$ at $T_N \approx 40$ mK, while for a sample with 6 at.% Ir doping no magnetic transition anomaly could be resolved at temperatures down to 0.02 K, suggesting that $\text{Yb}(\text{Rh}_{0.94}\text{Ir}_{0.06})_2\text{Si}_2$ is very close to the QCP [9]. Finally, $\text{Yb}(\text{Rh}_{0.83}\text{Ir}_{0.17})_2\text{Si}_2$ is on the paramagnetic side of the QCP [9]. Applying pressure of only $p = 0.46$ GPa on $\text{Yb}(\text{Rh}_{0.94}\text{Ir}_{0.06})_2\text{Si}_2$ is sufficient to shift the AFM transition up to $T_{N,H} \approx 0.14$ K. $T_{N,H}$ is clearly resolved as a kink in $\rho(T)$ (cf. figure 4a). A similar feature at the AFM transition has been observed in YbRh_2Si_2 [1]. With increasing pressure, $T_{N,H}(p)$ shifts to higher temperatures as expected for an Yb-based heavy fermion compound, but the signature of the transition in $\rho(T)$ is becoming less pronounced (figure 4b). At $p = 4.25$ GPa, a second more pronounced anomaly is appearing below $T_{N,H}$ at $T_{N,L} = 1$ K (indicated by an arrow in figure 4b). Two successive magnetic transitions have been also reported in YbRh_2Si_2 under pressure [7].

Electrical resistivity at low temperature follows a power-law dependence which can be expressed by $\rho(T) = \rho_0 + A_n T^n$. As displayed in the inset of figure 1, the temperature exponent $n = d \ln(\rho - \rho_0) / d \ln(T)$, remains nearly constant below $T = 1.5$ K with a value of $n \approx 1.0 \pm 0.1$. A recovery of a $\rho(T) / T^2$ behavior is not observed down to the lowest accessible temperature in our experiment. The resistivity exhibits a quasi-linear temperature dependence for all investigated pressures above $T_{N,H}$ characteristic of NFL behavior similar to that observed in the YbRh_2Si_2 . This suggests that disorder introduced by the substitution of Ir for Rh does not affect the quantum critical behavior strongly for this low Ir concentration. However, below the transition temperature $T_{N,L}$,

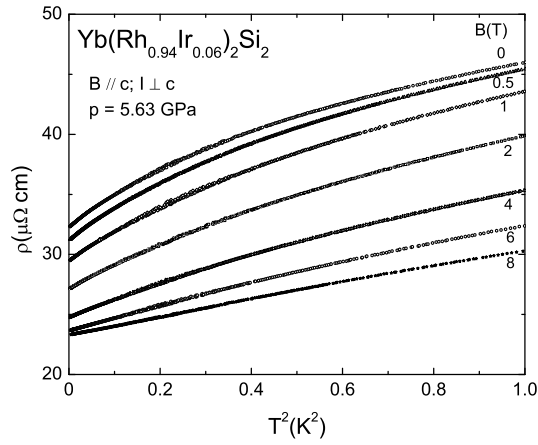


Figure 5. Temperature dependence of the resistivity ρ vs. T^2 at $p = 5.63$ GPa for different magnetic fields applied parallel to the direction of the crystallographic c axis.

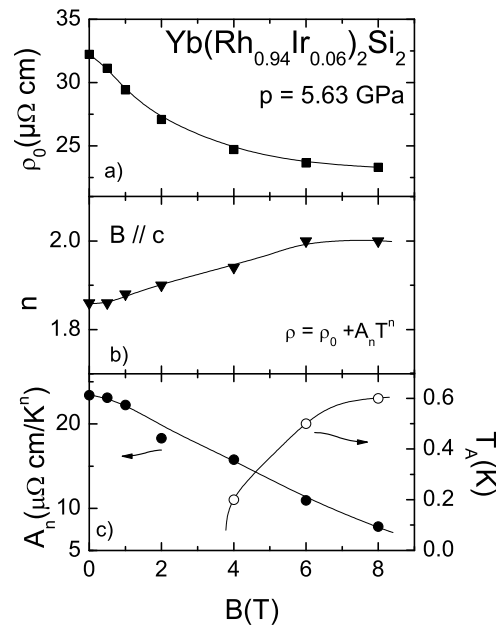


Figure 6. Magnetic field dependence of the residual resistivity ρ_0 (a), temperature exponent n (b), pre-factor A_n (c, left axis) obtained from a fit of $\rho = \rho_0 + A_n T^n$ to the low temperature resistivity data and T_A (c, right axis) upper limit of T^2 dependence of the resistivity at $p = 5.63$ GPa.

(T) can not be described by a T^2 dependence as in YbRh_2Si_2 [3].

At selected pressure, electrical resistivity has been measured in applied magnetic field. Figure 5 shows $\rho(T)$ of $\text{Yb}(\text{Rh}_{0.94}\text{Ir}_{0.06})_2\text{Si}_2$ as function of T^2 in different magnetic fields for $p = 5.63$ GPa. At this pressure in zero magnetic field $T_{N,\text{RH}} = 1.61$ K and

$T_{N, \mu H} = 0.9 \text{ K}$. Above $T_{N, \mu H}$, $\rho(T)$ follows a quasi-linear temperature dependence. It is interesting to note that at $B = 2 \text{ T}$, an anomaly can be still observed at about 1.3 K , but at $B = 8 \text{ T}$ no indication of any feature is visible in $\rho(T)$ anymore implying that magnetic order is suppressed at this magnetic field. In magnetic field the transition anomaly is broadened and, therefore, a complete analysis of the magnetic field dependence of the transition temperature is difficult. The resistivity data below $T = 0.6 \text{ K}$ can be described by a power-law behavior, $\rho(T) = \rho_0 + A_n T^n$. The magnetic field dependence of ρ_0 , n and temperature coefficient A_n for $p = 5.63 \text{ GPa}$ is plotted in figure 6. The residual resistivity, $\rho_0(B)$, is monotonically decreasing upon increasing magnetic field, but tends to saturate at large fields ($B = 6 - 8 \text{ T}$). While in small magnetic fields, $B = 2 \text{ T}$, a temperature exponent $n = 1.3$ significantly smaller than $n = 2$ as expected for a Landau Fermi liquid (LFL), is found, in magnetic fields $B \geq 4 \text{ T}$ the characteristic behavior of a LFL is recovered. The LFL region is growing in temperature with increasing magnetic field as can be seen by the extended linear region in the $\rho(T)$ vs. T^2 plot for large magnetic fields in figure 5. The field dependence of the crossover temperature giving the upper limit of the temperature range where the data can be described by a T^2 dependence is displaced in the figure 6c.

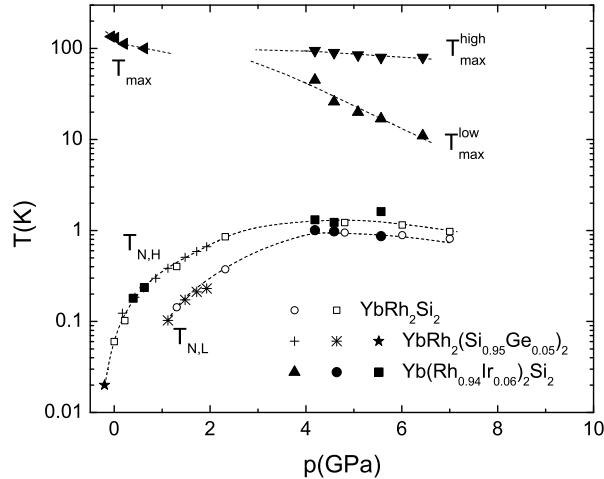


Figure 7. Temperature - pressure ($T - p$) phase diagram of $\text{Yb}(\text{Rh}_{0.94}\text{Ir}_{0.06})_2\text{Si}_2$ (solid symbols). Data of YbRh_2Si_2 (open symbols, Ref. [1, 7]) and $\text{YbRh}_2(\text{Si}_{0.95}\text{Ge}_{0.05})_2$ (crosses, Ref. [4]) have been included. (?): $T_{N, \mu H}$ of $\text{YbRh}_2(\text{Si}_{0.95}\text{Ge}_{0.05})_2$ at atmospheric pressure obtained from specific heat measurements (Ref. [3]). The data for $\text{Yb}(\text{Rh}_{0.94}\text{Ir}_{0.06})_2\text{Si}_2$ and $\text{YbRh}_2(\text{Si}_{0.95}\text{Ge}_{0.05})_2$ have been shifted by a fixed pressure of $p = 0.06 \text{ GPa}$ and $p = 0.2 \text{ GPa}$, respectively, with respect to YbRh_2Si_2 .

The $T - p$ phase diagram in figure 7 summarises the results obtained for $\text{Yb}(\text{Rh}_{0.94}\text{Ir}_{0.06})_2\text{Si}_2$. In addition, data for YbRh_2Si_2 [1, 7] and $\text{YbRh}_2(\text{Si}_{0.95}\text{Ge}_{0.05})_2$ [3, 4] are included. In the case of $\text{Yb}(\text{Rh}_{0.94}\text{Ir}_{0.06})_2\text{Si}_2$ the pressure axis has been shifted uniformly by $p = 0.06 \text{ GPa}$ and in the case of $\text{YbRh}_2(\text{Si}_{0.95}\text{Ge}_{0.05})_2$ by $p =$

0.2 GPa. As a result, the data for $T_{N,\text{H}}(p)$ and $T_{N,\text{L}}(p)$, respectively, for the different compounds collapse each on a single curve. The values of p are exactly the same like the ones obtained by calculating the equivalent chemical pressure induced by the lattice expansion due to the substitution. The equivalent pressure was calculated by using the lattice parameters obtained by X-ray diffraction and the bulk modulus of the pure sample ($B = 187$ GPa [5]). The expansion of the unit-cell volume of $\text{Yb}(\text{Rh}_{0.94}\text{Ir}_{0.06})_2\text{Si}_2$ compared with YbRh_2Si_2 by 0.03% can be translated in $\text{Yb}(\text{Rh}_{0.94}\text{Ir}_{0.06})_2\text{Si}_2$, being under an effective negative pressure of $p = -0.06$ GPa with respect to YbRh_2Si_2 . The very good agreement indicates that Ge and Ir substitution have mainly the effect of acting as chemical pressure and in addition shows that disorder effects play only a minor role. For La substitution on the Yb site a similar effect has been observed [17]. The existence of the low-moment AFM phase is a common feature for small Ge, La or Ir substitutions. The AFM ordering temperature, $T_{N,\text{H}}$, of $\text{Yb}(\text{Rh}_{0.94}\text{Ir}_{0.06})_2\text{Si}_2$ extrapolates to about $T_{N,\text{H}} = 20$ mK at ambient pressure consistent with magnetic susceptibility experiments in the temperature range $T > 20$ mK [9]. An extrapolation of $T_{N,\text{H}}(p)$ to zero temperature leads to a critical pressure $p_c = 0.25 - 0.05$ GPa.

4. Conclusion

In summary, we reported resistivity measurement on $\text{Yb}(\text{Rh}_{0.94}\text{Ir}_{0.06})_2\text{Si}_2$ under pressures up to $p = 6.5$ GPa in the temperature range 50 mK $< T < 300$ K. We could show that Ir substitution acts primarily as negative chemical pressure and disorder effects play only a minor role. The $T - p$ phase diagram of $\text{Yb}(\text{Rh}_{0.94}\text{Ir}_{0.06})_2\text{Si}_2$ and of pure YbRh_2Si_2 can be superimposed by shifting the pressure axis by $p = -0.06$ GPa. The data point to the existence of a pressure (volume) controlled QCP at $p_c = 0.25$ GPa. This suggests further Ir substitution studies to directly access the QCP at atmospheric pressure.

Acknowledgements

We would like to thank for the financial support of COST P16.

5. References

- [1] Trovarelli O, Geibel C, Mederle S, Langhammer C, Grosche FM, Gegenwart P, Lang M, Spam G and Steglich F 2000 Phys. Rev. Lett. 85, 626
- [2] Gegenwart P, Custers J, Geibel C, Neumaier K, Tayama T, Tenya K, Trovarelli O and Steglich F 2002 Phys. Rev. Lett. 89, 056042
- [3] Custers J, Gegenwart P, Wilhelm H, Tokiwa Y, Trovarelli O, Geibel C, Steglich F, Pepin C and Coleman P 2003 Nature 424, 524
- [4] Mederle S, Borth R, Geibel C, Grosche FM, Spam G, Trovarelli O and Steglich F 2002 J. Phys.: Condens. Matter 14, 10731
- [5] Plessel J, Abd-Elmeguid MM, Sanchez JP, Nebel G, Geibel C, Trovarelli O and Steglich F 2003 Phys. Rev. B 67, 180403R
- [6] Dionicio G, Wilhelm H, Spam G, Ferstl J, Geibel C and Steglich F 2005 Physica B 359-361, 50

- [7] Knebel G , Boursier R , Hassinger E , Lapertot G , Nicklowitz P G , Pourret A , Salce B , Sanchez J P , Shekin I , Bonville P , Harima H and Flouquet J 2006 J. Phys. Soc. Jpn. 75, 114709
- [8] Weickert F , Gegenwart P , Ferstl J , Geibel C and Steglich F 2006 Physica B 378-380, 72
- [9] Westerkamp T , Gegenwart P , Krellner C , Geibel C and Steglich F 2008 Physica B 1236-1238, 403
- [10] Stockert O , Kozma M M , Ferstl J , Murani A P , Geibel C and Steglich F 2006 Physica B 378-380, 15
- [11] Yuan H Q , Nicklas M , Hossain Z , Geibel C , and Steglich F 2006 Phys. Rev. B 74, 212403
- [12] Alam-Yadri K , Wilhelm H and Jaccard D 1998, Eur. Phys. J. B 6, 5
- [13] Yuan H Q , Grosche F M , Deppe M , Geibel C , Spam G and Steglich F 2003 Science 302, 2104
- [14] Rosch A 1999 Phys. Rev. Lett. 82, 4280
- [15] Miyake K and Narikiyo O 2002 J. Phys. Soc. Jpn. 71, 867
- [16] Miyake K and Maebashi H 2002 J. Phys. Soc. Jpn. 71, 1007
- [17] Nicklas M , Ferstl J , Geibel C and Steglich F 2006 Physica B 378-380, 159